

of resolution. If times available for observation are much shorter, image-amplification techniques or other diffraction methods (such as electron diffraction) must be used. In the case of rapid transformations of metastable alloy phases now under study (2), electron diffraction was difficult to use; a faster x-ray diffraction method was desired.

The polychromatic ("white") component of the x-radiation used in diffraction contributes to the continuous background of the diffraction pattern, along with inelastic scattering by the sample, fluorescence, and so on. The white component of the incident radiation undergoes coherent scattering (diffraction) by each crystal of the powder or sheet sample. Therefore the radiation scattered in any given direction contains information about the lattice, which is yielded by spectral analysis of the diffracted beam; with the aid of high-resolution semiconductor detectors, this analysis can be performed very quickly.

We combined a diffractometer having a Siemens x-ray source (Fe anode with

8 ma at 45 kv) with a lithium-drifted Si [Si(Li)] semiconductor detector connected to a 4096-channel pulse-height analyzer; use of such detectors for spectrography of *K* and *L* emission lines has been described (3).

The detection system included a TMC low-energy photon spectrometer (4) consisting of a Si(Li) detector (30 mm<sup>2</sup> by 3 mm) and a field-effect transistor preamplifier. The detector and the field-effect transistors were cooled in a liquid-nitrogen cryostat. Pulses from the preamplifier were passed through a Tennelec TC-200 amplifier before being analyzed and stored in a Packard 4096-channel pulse-height analyzer. The amplifier gain was adjusted so that the energy region between 0 and 64 keV was spread over a 1024-channel quadrant of the analyzer memory. The pulse-height-versus-energy curve (essentially linear) of the system was determined from spectra taken with standard sources of <sup>57</sup>Co and <sup>241</sup>Am (3); the full width at half-maximum (FWHM) of photopeaks produced by the standards varied from about 0.60 to

0.83 keV over the range 14 to 60 keV.

The geometric relation of source, diffracting sample, and detector was identical with that used in standard diffraction experiments, with the line normal to the specimen bisecting the angle (180 deg - 2θ) between the incident and diffracted beams. The diffractometer was set to a predetermined low angle (see below), and counts were taken for various periods with sheet samples of Cu, Ag, Re, Pt, and Au.

Figure 1a shows a diffraction pattern of Pt sheet; all diffraction peaks up to (333/511) are present and resolvable, and the Pt *L*-radiation is resolved into α, β, and γ peaks. The similarity to a conventional powder diffraction pattern of a face-centered-cubic (fcc) material is immediately obvious if one considers a slight (100)[001] cube texture of the Pt sheet, which enhances the (200) and (400) reflections. The FWHM values of the peaks (Fig. 1a) are slightly greater than the values quoted above because of the contribution of slit width in the case of diffraction peaks and because of multiple components for the fluorescence peaks.

The upper curve (Fig. 1b) represents the response of the detector to the undiffracted primary beam. The observed response function  $I_R(E)$  is determined by two factors:

$$I_R(E) = I_{\text{cont}}(E) \cdot P_a(E) \quad (2)$$

where  $I_{\text{cont}}(E)$  is the intensity of emitted white radiation of energy  $E$ , and  $P_a(E)$  is the probability of photopeak absorption of photons of energy  $E$  by the detector. One sees that  $I_R(E)$  has a maximum at about  $E = 19$  keV and falls off rapidly at lower energies [because of reduction in  $I_{\text{cont}}(E)$  and  $P_a(E)$ , in the latter because of such factors as absorption in the cryostat window] and at higher energies [because of reduction in  $P_a(E)$ ]. Note that in Fig. 1b the high-energy tail of the  $I_R(E)$  distribution extends above the cutoff of the x-ray tube (45 keV) because of some pileup of pulses as a result of the high count rate from the direct beam; this effect is not present in the diffraction patterns, which were taken at much lower count rates.

The shape of  $I_R(E)$  is superimposed over the diffraction pattern given by the customary x-ray crystallographic treatment; the shape of  $I_R(E)$  causes the low intensity of the high-energy lines, especially (422) and (333/511), prior to the high-energy cutoff at 45 keV.

For evaluation of the  $d$ -spacings from

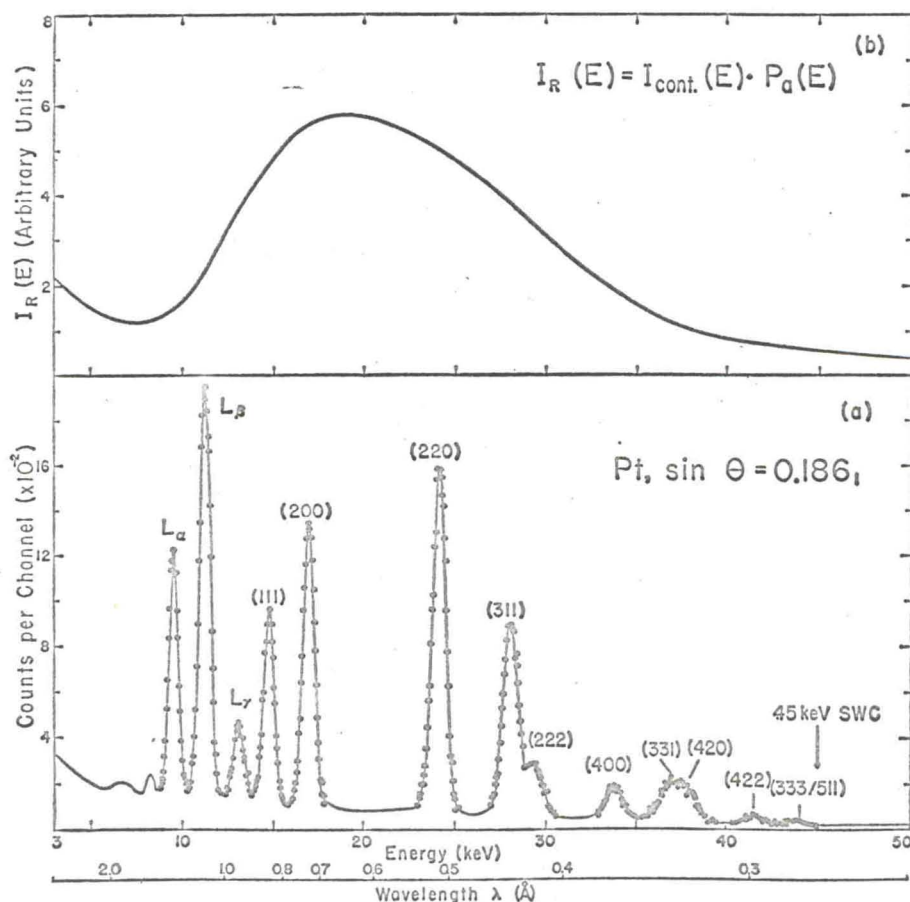


Fig. 1. (a) Diffraction pattern and *L*-fluorescence spectrum of platinum sheet, obtained by x-ray spectroscopy; SWC, shortwave cutoff of x-ray beam. (b) Response of detector to undiffracted polychromatic x-ray beam.